JLB

Article

SIRT1 inhibition during the hypoinflammatory phenotype of sepsis enhances immunity and improves outcome

Vidula T. Vachharajani,[*,1] Tiefu Liu,[†] Candice M. Brown,[†] Xianfeng Wang,[*] Nancy L. Buechler,[*] Jonathan David Wells,[‡] Barbara K. Yoza,[†,‡] and Charles E. McCall[†]*

Departments of *Anesthesiology, [†]Internal Medicine, and [‡]Surgery, Wake Forest School of Medicine, Winston-Salem, North Carolina, USA

RECEIVED JANUARY 17, 2014; REVISED JUNE 13, 2014; ACCEPTED JUNE 16, 2014. DOI: 10.1189/jlb.3MA0114-034RR

ABSTRACT

Mechanism-based sepsis treatments are unavailable, and their incidence is rising worldwide. Deaths occur during the early acute phase of hyperinflammation or subsequent postacute hypoinflammatory phase with sustained organ failure. The acute sepsis phase shifts rapidly, and multiple attempts to treat early excessive inflammation have uniformly failed. We reported in a sepsis cell model and human sepsis blood leukocytes that nuclear NAD+ sensor SIRT1 deacetylase remodels chromatin at specific gene sets to switch the acute-phase proinflammatory response to hypoinflammatory. Importantly, SIRT1 chromatin reprogramming is reversible, suggesting that inhibition of SIRT1 might reverse postacute-phase hypoinflammation. We tested this concept in septic mice, using the highly specific SIRT1 inhibitor EX-527, a small molecule that closes the NAD+ binding site of SIRT1. Strikingly, when administered 24 h after sepsis, all treated animals survived, whereas only 40% of untreated mice survived. EX-527 treatment reversed the inability of leukocytes to adhere at the small intestine MVI, reversed in vivo endotoxin tolerance, increased leukocyte accumulation in peritoneum, and improved peritoneal bacterial clearance. Mechanistically, the SIRT1 inhibitor restored repressed endothelial E-selectin and ICAM-1 expression and PSGL-1 expression on the neutrophils. Systemic benefits of EX-527 treatment included stabilized blood pressure, improved microvascular blood flow, and a shift toward proimmune macrophages in spleen and bone marrow. Our findings reveal that modifying the SIRT1 NAD+ axis may provide a novel way to treat sepsis in its hypoinflammatory phase. *J. Leukoc. Biol.* 96: 785–796; 2014.

Abbreviations: APC=allophycocyanin, CLP=cecal ligation and puncture, Dv=venular diameter, fl/fl=flox/flox, MM=intravital microscopy, LA=leukocyte adhesion, Lys-Cre=lysozyme Cre, MAP=mean arterial pressure, MDSC=myeloid-derived suppressor cell, MFI=mean fluorescence intensity, MSKO=myeloid-specific sirtuin 1 knockout, MVI=microvascular interface, NAD+=oxidized nicotinamide adenine dinucleotide, NS=normal saline, PMN=polymorphonuclear, PSGL-1=P-selectin glycoprotein ligand-1, SIRT1=sirtuin 1, Vplt=velocity of noninteracting and free-flowing platelets, VWF=Von Willebrand factor, WSR=wall shear rate, WT=wild-type

Introduction

Sepsis incidence is rising, despite the efforts for early detection [1]. The excessive acute inflammatory host response of sepsis switches to hypoinflammation, leading to immunosuppression during postacute phase. Whereas a small minority of patients may benefit from early anti-inflammatory therapies during acute sepsis, most patients who survive the initial inflammatory onslaught remain in intensive care units with multiorgan failure during the postacute hypoinflammatory and repressed adaptive-immunity phase, which exist during most deaths from sepsis [2, 3]. Most mechanism-based therapies studied so far targeted the acute phase and were uniformly unsuccessful [4]. As the initial inflammatory onslaught is replaced quickly by a hypoinflammatory phase, there is a dire need for phase-specific treatment for septic patients.

Most studies of post-acute sepsis with immunosuppression have emphasized altering adaptive immunity [5–8]. There are no studies, to our knowledge, focusing on leukocyte-endothelial interactions at the MVI in this setting. The MVI connects the systemic circulation and local tissue environment and directs the systemic inflammatory stimulus by delivering leukocytes to the local tissue [9]. This early step is essential for mounting the innate immune response during all types of physiologic and pathophysiologic responses to environmental threats, including sepsis [10, 11]. It is not surprising that there is a direct correlation between endothelial cell activation, especially cell adhesion biomarkers, and sepsis mortality [12]. We previously reported increased LA at the MVI in early sepsis [11], but temporal changes in microvascular LA during sepsis progression (in a given model of sepsis) are poorly characterized. Also, how repressed LA at the MVI contributes to reduced innate immunity during the hypoinflammatory phase and whether in vivo endotoxin tolerance contributes to repressed MVI responses during sepsis are unclear.

Endotoxin tolerance was first described by Beeson [13] as a decreased response to endotoxin-induced fever after typhoid

1. Correspondence: Dept. of Anesthesiology, Wake Forest School of Medicine, Winston-Salem, NC 27157, USA. E-mail: vvachhar@wakehealth.edu

vaccine injections in rabbits in 1947. It commonly occurs in human and animal sepsis and when present ex vivo, marks the shift from the proinflammatory phase to a hypoinflammatory response [14–16]. We have shown previously that NAD+-dependent activation of class III histone deacetylase SIRT1 coordinates the acute inflammatory response and development of endotoxin tolerance in human monocytic cells ex vivo and in blood leukocytes during human sepsis by epigenetically reprogramming innate immune and metabolic pathways [17, 18]. We found further that the chromatin repressor switch required NF-κB factors RelA/p65 and RelB, histone deacetylases, and histone and DNA methyl transferases [14, 19]. We determined further that nuclear SIRT1 activation by NAD+ is necessary and sufficient for generating endotoxin tolerance. More importantly, we have also reported that endotoxin tolerance can be reversed in vitro by inhibiting SIRT1 activity pharmacologically or genetically [18].

In the current study, we used in vivo endotoxin tolerance as a marker in septic mice to identify three temporally controlled phenotypes at the MVI, the acute hyperinflammatory, postacute hypoinflammatory, and resolution. Based on our published in vitro studies [17, 18], we hypothesized that reducing SIRT1 activity before it has countered the acute hyperinflammatory response and before its epigenetic shift to hypoinflammation would worsen sepsis outcome; in contrast, the inhibition of the increased SIRT1 expression of the hypoinflammatory phase of the sepsis responses would improve sepsis outcome and promote resolution by rebalancing innate immune homeostasis. We studied this by testing effects of the highly specific SIRT1 inhibitor (EX-527) on sepsis MVI over the course of the early hyper- and late hypoinflammatory phases. We found that SIRT1 inhibition during the first 12 h of sepsis further increased LA at the MVI and substantially reduced survival. The effect of low SIRT1 on MVI was substantiated by increased LA in myeloid-specific SIRT1-deficient mice. In striking contrast, inhibition of SIRT1 24 h after sepsis onset, when endotoxin tolerance with hypoinflammation had set in at the MVI, increased LA, reversed paralysis of LA, improved innate immune responses in spleen and peritoneum, increased the rate of bacterial clearance in peritoneum, improved cardiovascular function, and markedly reduced sepsis-associated mortality.

MATERIALS AND METHODS

Animals

This study was approved by the Institutional Animal Care and Use Committee of the Wake Forest School of Medicine and was performed according to National Institutes of Health guidelines. The WT mice (C57Bl/6) were purchased from The Jackson Laboratory (Bar Harbor, ME, USA). MSKO and control SIRT1 knockout mice breeding pairs were obtained from Dr. Hang Shi (Georgia State University, Atlanta, GA, USA), and mice were bred in an Association for Assessment and Accreditation of Laboratory Animal Care-approved facility at Wake Forest School of Medicine. MSKO mice were created by crossing SIRT1 fl/fl mice (backcrossed with C57Bl/6 for six generations) with the SIRT1 allele containing a LoxP-floxed exon 4 (The Jackson Laboratory) with Lys-Cre mice (The Jackson Laboratory) with Cre expression in myeloid lineage cells, including macrophages and monocytes. Initially, we generated WT, homozygous SIRT1 fl/fl, Lys-Cre, and MSKO mice. If there was no difference in the inflammatory phenotypes among the three control groups (WT, fl/fl, and Lys-Cre), then we used the MSKO and their littermates fl/fl mice in the study.

LPS responsiveness was determined using *Escherichia coli* LPS (O111:B4 LPS: 5 μg/mouse i.p., 4 h of stimulation). EX-527(Cayman Chemical, Ann Arbor, MI, USA) stock solution in DMSO was prepared (2.5 mg/ml). Mice were injected with EX-527, 10 mg/kg (4 ml/kg), or an equivalent volume of DMSO (4 ml/kg) i.p. at indicated time-points. This dose of EX-527 in mice was as per documented literature [20].

CLP

Sepsis was induced using CLP as described in the literature [11, 21]. After ligation, cecum was perforated two times with a 22-gauge needle, contents were returned, and abdominal incision was closed in two layers (peritoneum and skin). Fluid resuscitation (NS 1 ml s.c.) was given to each mouse. The Sham-operated mice underwent laparotomy and fluid resuscitation, as described above, without cecal ligation or puncture. Mice with CLP (Sepsis) and Sham surgeries were used for tissue harvest (peritoneal lavage, spleen and bone marrow-derived cells, small intestinal tissue) or video IVM.

Fluorescent IVM

At indicated time-points after CLP/Sham surgery, the mice underwent carotid artery and jugular venous cannulations, and small intestinal microcirculation was studied (n=4–6 mice/group) using the Nikon Eclipse FN1 microscope (Nikon Instruments, Melville, NY, USA), as described previously [11, 22]. Mice were injected with rhodamine G (0.02% in 100 μl PBS) for leukocyte visualization, while platelets were labeled green ex vivo with CFSE (90 μM).

Circulating cell–endothelial cell interactions

To visualize interactions between leukocytes/platelets and venular endothelium in the mouse small intestine, leukocytes were labeled red in vivo by injecting i.v. rhodamine 6G (Sigma-Aldrich, St. Louis, MO, USA; 0.02% in 100 μl PBS), whereas platelets were labeled green ex vivo with CFSE (Sigma-Aldrich; 90 μM). This allowed simultaneous monitoring of both cell types in each venule. The details of the platelet-isolation technique are as outlined previously [11]. Contamination of the platelet suspension by leukocytes was evaluated from a 25-μl sample to ensure that the leukocyte count did not exceed 0.01%. The platelets (n=100×10^6) were infused i.v. for over 5 min (yielding <5% of the total platelet count) and allowed to circulate for a period of 5 min before recording on a DVD. Evidence suggests that these platelet-isolation procedures have no significant effect on the activity or viability of isolated platelets [23].

Postcapillary venules (three to five in number; five to seven mice/group) in each mouse intestine were recorded to quantify leukocyte and platelet adhesion, and each recording was analyzed for 1 min. A circulating cell (leukocyte/platelet) was considered adherent if it remained stationary for at least 30 consecutive s of the 1-min recording. The mean of the average values of LA determined in each mouse was then used to generate a group mean.

Recordings were reanalyzed for the platelet velocity. Only the noninteracting platelets (with the endothelium/leukocyte/other platelets) were used to assess platelet velocity. Estimates of pseudo-shear rate in venules were obtained using measurements of Dv and the maximal Vplt, according to the following formulation: pseudo-shear rate = [(Vplt/1.6)/Dv] × 8/s [24]. Venular WSRs are important to elucidate the effect of venular WSRs on leukocyte/platelet adhesion in microcirculation of different groups of mice.

Immunohistochemistry of small intestinal tissue

Small intestinal tissue was harvested and frozen using Optimal Cutting Temperature medium. Acetone-fixed, frozen sections of tissue were stained using primary SIRT1, E-selectin, ICAM-1, and VWF antibodies and fluores-

cently labeled secondary antibodies. Antibodies used and image acquisitions are described below.

Primary antibodies. Primary antibodies included SIRT1 (Santa Cruz Biotechnology, Santa Cruz, CA, USA), VWF antibodies (Abcam, Cambridge, MA, USA), and E-selectin and ICAM-1 antibodies from BD Biosciences (San Jose, CA, USA).

Secondary antibodies. Cy3-conjugated, labeled secondary antibodies for SIRT1, E-selectin, and ICAM-1 and FITC-conjugated secondary antibody for VWF secondary antibody were purchased from Jackson ImmunoResearch Laboratories (West Grove, PA, USA).

Image acquisition. Virtual images were captured with an Olympus VS110 (20×/0.75 objective; Olympus, Center Valley, PA, USA). Static images were captured using OlyVIA (Olympus) at the designated magnification. Camera is an Olympus XM10.

Tissue immunoblots

Mouse small intestine tissue lysate was prepared by homogenization in modified radioimmunoprecipitation assay buffer (150 mM NaCl, 50 mM Tris-HCl, pH 7.4, 1 mM EDTA, 1 mM PMSF, 1% Triton X-100, 1% Na deoxycholic acid, 0.1% SDS, plus protease inhibitor and phosphatase inhibitor cocktails). Tissue and cell debris were removed by centrifugation at 13,000 rpm for 30 min after sonication. Protein concentration was determined with Bio-Rad DC protein assay and adjusted into the same value. The tissue lysate was boiled for 5 min in 1× SDS sample buffer (50 mM Tris-HCl, pH 6.8, 12.5% glycerol, 1% sodium dodecylsulfate, 0.01% bromophenol blue) containing 5% β-mercaptoethanol. The same amount of protein lysate was resolved by SDS-PAGE as before [25], and protein levels were measured by immnoblotting. GAPDH was used as loading control. The membrane was blocked and then incubated with SIRT1 antibody (07–131, 1:1000; Millipore, Billerica, MA, USA) and GAPDH antibody (AM4300, 1:15000; Invitrogen, Carlsbad, CA, USA), respectively, overnight in a cold room. The blots were incubated with Alexa Fluor 680-conjugated secondary antibodies (827–10080 and 827–10081, 1:10,000; LI-COR Biosciences, Lincoln, NE, USA) on the 2nd day. The signal was developed with a Li-COR Odyssey Infrared Imager system (Li-COR Biosciences).

Isolation and treatment of splenocytes, peritoneal cells, and bone marrow

The mice were injected with vehicle or EX-527 (24-h sepsis), and whole blood, splenocytes, bone marrow, and peritoneal cells were isolated at indicated time-points. Splenocytes and MDSCs were stimulated with LPS (1 μg/ml vs. NS) and incubated for 1 h for mRNA expression and 24 h for protein expression of cytokines. Whole blood, peritoneal cells, splenocytes, and bone marrow-derived cells were also subjected to flow cytometry. Peritoneal lavage fluid also was assessed for bacterial burden. Details of whole blood leukocyte, splenocyte, peritoneal, and bone marrow-derived cell flow cytometry and peritoneal lavage bacterial clearance are described below.

Flow cytometry

Peritoneal lavage cells, splenocytes, or bone marrow cells (1–2×10^6 cells) in FACS buffer (eBioscience, San Diego, CA, USA) were incubated with anti-mouse CD16/CD32 for 10 min (4°C), followed by a 1-h incubation (4°C) with conjugated antibodies, isotype-labeled controls, or OneComp eBeads as compensation controls. Antibodies were: anti-mouse CD11b-APC, anti-mouse F4/80-PE, anti-mouse Ly-6C PerCP-Cy5.5, anti-mouse Ly-6G (Gr-1)-PE, and anti-mouse Ly-6G-FITC (BD Biosciences); all reagents were from eBioscience unless stated otherwise. Stained cells were fixed in 0.1% paraformaldehyde for 10 min and stored in PBS until FACS analysis. Stained cells and compensation controls were analyzed using a FACSCalibur (BD Biosciences) and BD CellQuest Pro software (bone marrow) or an Accuri C6 cytometer and CFlow Plus analysis software (BD Biosciences) for peritoneal macrophages and splenocytes; further data analysis was performed using FlowJo 10.0.4 software (Treestar, Ashland, OR, USA). Peritoneal lavage cells (1–2×10^6 cells) in FACS were incubated with anti-mouse CD16/CD32 for 10 min (4°C), followed by a 1-h incubation (4°C) with conjugated antibodies, isotype-labeled controls, or OneComp eBeads as compensation controls. Antibodies were: anti-mouse CD11b-APC, anti-mouse F4/80-PE, anti-mouse Ly-6C PerCP-Cy5.5, anti-mouse Ly-6G (Gr-1)-PE, and anti-mouse Ly-6G-FITC (BD Biosciences); all reagents were from eBioscience unless stated otherwise. Stained cells were fixed in 0.1% paraformaldehyde for 10 min and stored in PBS until FACS analysis using a FACSCalibur (BD Biosciences). Data analysis was performed using FlowJo 10.0.4 software (Treestar).

Whole blood leukocytes: After blood collection from carotid arterial cannulation, peripheral leukocytes were stained with anti-CD45 (eBioscience) and anti-PSGL-1 (BD Biosciences) antibodies, and samples were assayed by flow cytometry using a BD Accuri C6 flow cytometer (BD Biosciences). We gated for total leukocytes and neutrophil subset by side-scatter for CD45+ and PSGL-1+ cells. The samples were then analyzed using CFlow Plus analysis software (BD Biosciences) and the MFI of PSGL-1 expression in CD45+-gated total leukocytes and granulocytes was determined. MFI values were normalized to sham control. Data are expressed as fold of control (see Fig. 7).

Bone marrow harvest and MDSC isolation

Bone marrow cells were harvested by flushing femurs and tibias with cold PBS. Red blood cells in the cell suspension were lysed using 1 ml ammonium-chloride-potassium buffer (Lonza, Allendale, NJ, USA), quenched with 10 vol cold PBS, and centrifuged at 165 *g*. The cell suspension was washed two additional times. Two enriched populations of MDSCs, Gr1+/Ly6G+ and Gr1+/Ly6G−, were isolated in the bone marrow cell suspension with a MDSC Isolation Kit (Miltenyi Biotec, Auburn, CA, USA), according to the manufacturer's instructions. Enriched cell populations were resuspended in RPMI-1640 medium. For ex vivo MDSC treatment, Gr1+/Ly6G+ and Gr1+/Ly6G− cells were plated at 0.5 ×10^4–1 × 10^5 cells/well in a 96-well plate and stimulated with NS or LPS (1 μg/ml, *E. coli* O55:B5) for 24 h at 37°C/5% CO_2. All media were collected after 24 h and stored at −20°C. Cells remaining in wells were washed with cold PBS, lysed with 1% Tween 20, and stored at −20°C for total protein quantification by bicinchoninic acid (Pierce, Rockford, IL, USA). Following quantification of secreted TNF-α by ELISA, the TNF-α concentration in each well was normalized to total protein concentration. TNF-α media concentrations were quantified using the mouse TNF-α ELISA Ready-SET-Go! kit (eBioscience).

RNA extraction and RT-PCR

RNA was extracted using TRI Reagent (Molecular Research Center, Cincinnati, OH, USA). The mRNA expression levels of target genes were quantified by quantitative real-time PCR with a one-step method, as described previously [25]. The total RNA concentration was adjusted to 100 ng/μL, and 10 ng total RNA was loaded for real-time PCR in 25 μl total volume. The RT-PCR was carried out at 48°C for 30 min, followed by 95°C for 10 min, and then 40 cycles at 95°C for 15 s and 60°C for 1 min. All results were normalized to GAPDH RNA levels. Relative quantification was calculated using the ΔΔ comparative threshold formula. All samples were run in quadruplicates. The average and SE values were calculated. TaqMan primer/probes for mouse GAPDH, TNF-α, and IL-1β were purchased from Invitrogen (Grand Island, NY, USA).

Assessment of peritoneal bacterial burden

Peritoneal lavage was performed (described above). Peritoneal fluid was then diluted by sixfold with lysogeny broth medium (Luria-Bertani broth base) and cultured in a 37°C shaker for 5 h, the time required for most bacterial cultures to reach log growth phase. Bacterial quantity was evaluated by optical density at the wavelength 600 nm using the Infinite M200 reader (Tecan, San Jose, CA, USA).

Statistics

All data were analyzed using GraphPad Prism 6.0 (GraphPad Software, La Jolla, CA, USA). Analyses between two population means were analyzed

using unpaired, two-tailed Student's *t*-test or Mann-Whitney test for nonparametric data sets; analyses with more than three samples were analyzed using one-way ANOVA or two-way ANOVA with Tukey's post hoc comparisons as appropriate. $P < 0.05$ was designated as significant. LA in different groups was analyzed using Tukey-Kramer post hoc analysis (StatView; SAS Institute, Cary, NC, USA). $P < 0.05$ was designated as significant. Log rank test was used to compare survival between the groups in the Kaplan-Meier survival curves, and $P < 0.05$ was designated as significant.

RESULTS

LA in sepsis microcirculation is disrupted during endotoxin tolerance

Polymicrobial sepsis increases LA in the microvasculature of mice [11, 22, 26], but whether LPS tolerance (marker for immunosuppression) occurs in vivo in the microvasculature is unknown. To test this and identify phases of sepsis, we challenged septic mice with LPS/vehicle (NS) at different timepoints and quantified in vivo LA, 4 h after each LPS challenge. **Figure 1A** shows that peak LA in the postcapillary venules of the small intestine occurred at 12 h and decreased 18 h after sepsis onset. LPS challenge enhanced sepsis-induced LA early, up to 12 h of sepsis (hyperinflammatory phase), but at 18 h, microvascular LA was LPS-tolerant, and this state persisted for at least 36 h (hypoinflammatory phase). By 72 h and up to 7 days after sepsis induction, LA response to LPS challenge returned toward levels seen in pre-endotoxin tolerant sepsis (putative resolution phase). From these results, we identified timepoints to test effects of EX-527 treatment of sepsis.

Low SIRT1 regulates the acute hyperinflammatory-phase responses of sepsis

Low basal levels of SIRT1 occur in chronic states of inflammation, such as obesity with metabolic syndrome, and promote a proinflammatory state [27]. To clarify whether low SIRT1 regulates the acute hyperinflammatory-phase response of septic mice, we tested whether SIRT1 inhibition increased LA in mice pretreated with EX-527 before CLP. Figure 1B shows marked increases in LA in 6 h with the Sepsis group (hyperinflammatory phase) with EX-527 pretreatment. These results support that pretreatment with SIRT1 inhibitor accentuates the acute proinflammatory phenotype of sepsis.

To clarify further the effect of decreased SIRT1 on microvascular inflammation during sepsis, we studied LA in MSKO versus littermate control mice with CLP during the hyperinflammatory phase of sepsis. As shown in Fig. 1C, there was a significant increase in LA in MSKO compared with littermate WT control mice with sepsis.

SIRT1 expression increases in small intestinal villi during the hypoinflammatory phase of sepsis

To examine SIRT1 expression and effect of SIRT1 inhibition during the hypoinflammatory phase (24-h postsepsis) on the small intestine, we performed immunohistochemistry in small intestinal tissue of Sepsis mice with and without EX-527 treatment. As shown in **Fig. 2A**, SIRT1 expression increased in small intestinal villi in Sepsis versus Sham mice, and EX-527 reduced SIRT1 expression. The images support that enterocytes and microvasculature increase SIRT1 expression.

We then examined the SIRT1 expression in the small intestinal tissue using immunoblotting in Sham, Sepsis + Vehicle, and Sepsis + EX-527-treated mice (Fig. 2B). Representative samples from these groups show that whereas there was an increase in SIRT1 expression in Sepsis + Vehicle and Sepsis + EX-527 groups, there was no difference in SIRT1 expression in Sepsis + EX-527 versus Sepsis + Vehicle groups.

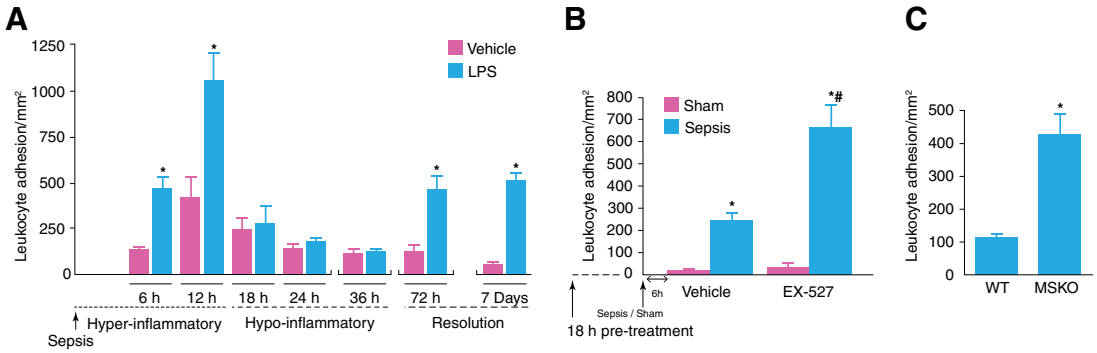

Figure 1. (A) LA in sepsis microcirculation exhibits endotoxin tolerance. LA in small intestinal microcirculation (mice, n=5/group) measured using IVM peaked at 12 h in the Vehicle (NS) group and decreased after 18 h in the Sepsis (CLP) group. LA in response to LPS restimulation increased significantly further (vs. Vehicle) in 6- and 12-h Sepsis groups (hyperinflammatory), whereas it did not in 18-, 24-, and 36-h Sepsis groups, indicating endotoxin tolerance (immunosuppression). Microvascular responsiveness returned in the 72-h Sepsis group (resolution; n = 4–6/group). *$P < 0.05$ versus respective Vehicle group Tukey's post hoc analysis; error bars: SEM. (B and C) Low SIRT1 increases the inflammatory responses in early sepsis. We studied the effect of SIRT1 deficiency on sepsis using two different strategies as follows: (B) SIRT1 inhibitor EX-527 pretreatment in WT mice (n=5–6/group); mice were pretreated (18-h pre-CLP) with EX-527 or Vehicle and LA measured in small intestinal microcirculation after 6 h Sepsis/Sham (hyperinflammatory phase). LA of the Sepsis + EX-527 group was increased significantly compared with Sepsis + Vehicle. *$P < 0.05$ versus respective Sham; #$P < 0.05$ versus Sepsis + Vehicle (Tukey's post hoc analysis; error bars: SEM). (C) Sepsis in MSKO (n=5/group); LA in MSKO mice was increased 6 h after sepsis compared with littermate WT control mice with sepsis. *$P < 0.05$ versus WT; Tukey's post hoc analysis; error bars: SEM.

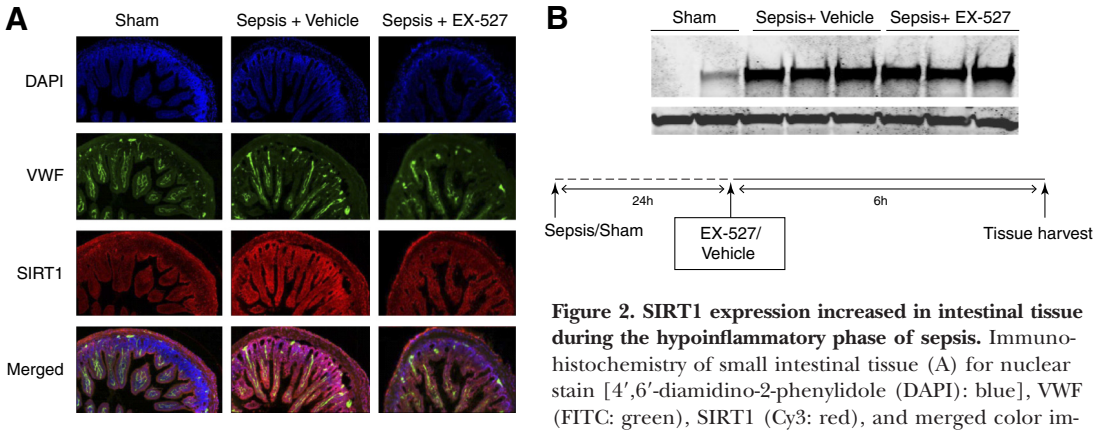

Figure 2. SIRT1 expression increased in intestinal tissue during the hypoinflammatory phase of sepsis. Immunohistochemistry of small intestinal tissue (A) for nuclear stain [4′,6′-diamidino-2-phenylidole (DAPI): blue], VWF (FITC: green), SIRT1 (Cy3: red), and merged color image shows that SIRT1 expression increased in 30-h Sepsis + Vehicle compared with Sham control. SIRT1 expression decreased in the Sepsis + EX-527 group versus Sepsis + Vehicle. Immunoblotting of small intestinal tissue (B) shows that there was an increase in SIRT1 expression in the small intestinal tissue compared with sham control. There was no difference in SIRT1 expression between Sepsis + Vehicle versus Sepsis + EX-527 groups using immunoblots.

EX-527 treatment during the hypoinflammatory phase of sepsis restores the microvascular response in vivo

Based on our results showing that EX-527 treatment increases LA, we hypothesized that EX-527 treatment during the hypoinflammatory phase (24-h sepsis) increases LA and/or restores microvascular responsiveness to LPS. We treated mice with EX-527 (test cohort) or vehicle (control), 24 h after CLP (denoted as Sepsis). We then studied LA in small intestinal microcirculation, 6-h post-treatment (30-h postsepsis). We found that LA was increased significantly in EX-527-treated septic mice (**Fig. 3A** and **B**; sepsis alone). We next determined the effect of in vivo LPS challenge on LA in EX-527-treated septic mice, predicting that LPS tolerance would be reversed by the treatment. We found that the microvascular response to LPS increased significantly after EX-527 treatment (Fig. 3A and B; Sepsis+LPS), whereas vehicle-treated mice remained LPS-tolerant. These data support that EX-527 treatment shortens the hypoinflammatory phase in rodent sepsis.

To ascertain whether the effect of EX-527 treatment is transient or sustained, we tested the effect of EX-527 treatment on LA, up to 48-h post-treatment (72-h Sepsis). As shown in **Fig. 4**, we observed that the increased LA in EX-527-treated mice with sepsis is sustained at least up to 72 h.

EX-527 improves systemic vascular responses

Sepsis causes profound changes in cardiovascular and microvascular function [10, 11]. To examine systemic inflammatory vascular responses, we measured MAP (mmHg) and pseudo-WSR (s^{-1}) as indices of blood flow in the microcirculation of

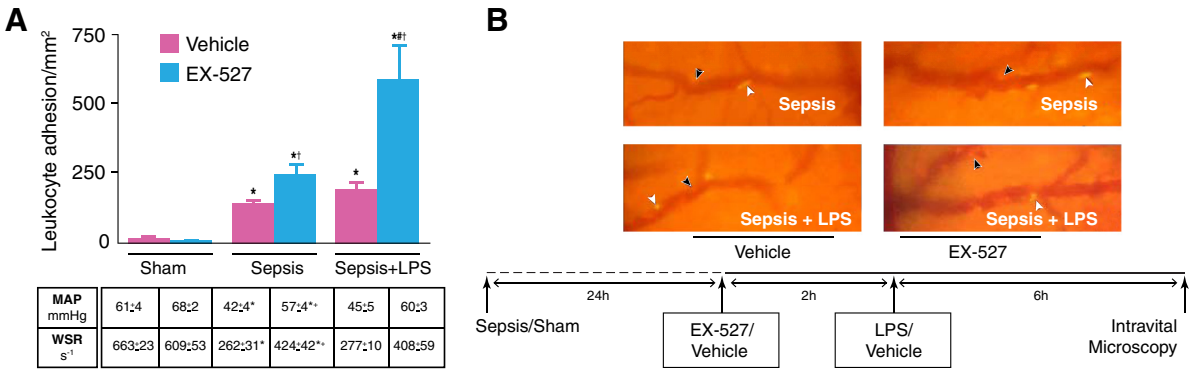

MAP mmHg	61±4	68±2	42±4*	57±4*‡	45±5	60±3
WSR s^{-1}	663±23	609±53	262±31*	424±42*‡	277±10	408±59

Figure 3. (A) EX-527 reverses microvascular endotoxin tolerance in mice. Small intestinal microvasculature IVM in mice treated with EX-527 versus Vehicle (30-h Sepsis; 6-h post-treatment; n=5–6/group) shows significantly increased LA in the Sepsis + EX-527 group, given LPS restimulation, whereas the Sepsis + Vehicle group remained LPS-tolerant. LA in LPS-stimulated and unstimulated Sepsis + EX-527 groups was increased significantly versus respective Sepsis + Vehicle. The table (lower) shows increased MAP (mmHg) and pseudo-WSR (s^{-1}) in Sepsis + EX-527 versus Sepsis + Vehicle. *$P < 0.05$ versus Sham + respective treatment; #$P < 0.05$ versus Sepsis + respective treatment; †$P < 0.05$ versus Sepsis + Vehicle; ‡$P < 0.05$ versus Sepsis + Vehicle + LPS. (B) Representative photomicrographs of small intestinal postcapillary venules in Vehicle and EX-527-treated mice stimulated further with LPS (lower) or vehicle (upper) show a significantly higher number of leukocytes (orange, filled arrowheads) adherent in EX-527-treated mice versus Vehicle-treated counterparts (open arrowheads show platelets, green).

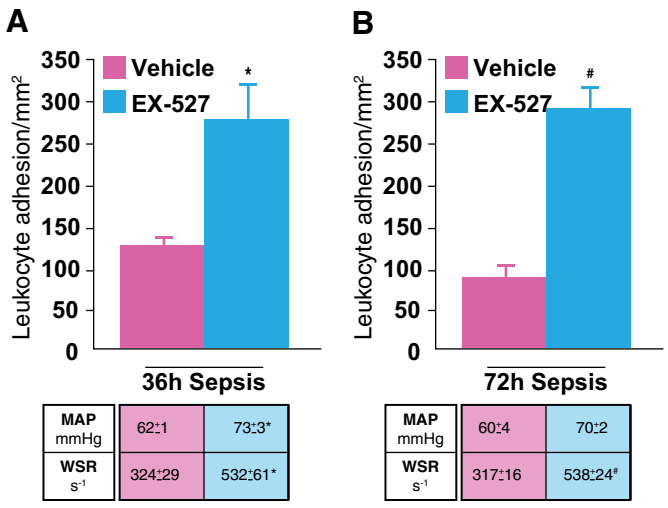

Figure 4. Increased LA in EX-527-treated sepsis mice is sustained into resolution phase. LA in small intestinal microvasculature in Sepsis mice (n=5–6/group) given EX-527 or Vehicle in 36-h Sepsis (12-h post-treatment; A) or 72-h Sepsis (48-h post-treatment; B) is significantly elevated at both time-points. The tables (lower) show that the EX-527 group exhibited increased MAP (mmHg) versus Vehicle in 36-h Sepsis, whereas WSR (s^{-1}) in EX-527-treated mice remained elevated at both time-points. *$P < 0.05$ versus Sepsis + Vehicle 36-h group; #$P < 0.05$ versus Sepsis + Vehicle 72-h group (Tukey's post hoc analysis; error bars: SEM).

septic mice treated with or without EX-527. We found that EX-527 treatment significantly increased MAP and WSR in Sepsis alone and in Sepsis + LPS (Fig. 3A) versus vehicle-treated counterparts. Additionally, a persistent effect of EX-527 treatment on MAP and WSR was observed at 36 h and 72 h after sepsis (Fig. 4). These results support that EX-527 has the systemic effect of improving blood pressure and blood flow to the organs during sepsis.

EX-527 treatment increases endothelial activation during the hypoinflammatory phase

Increased LA in EX-527-treated mice during the hypoinflammatory phase of sepsis may be a result of endothelial or circulating cell activation or both. To elucidate endothelial activation further, we examined E-selectin and ICAM-1 expression in small intestinal tissue using immunohistochemistry in EX-527 versus Vehicle-treated mice. As shown in **Figs. 5** and **6**, E-selectin and ICAM-1 expressions in small intestinal tissue increased in the hyperinflammatory phase (6 h) of sepsis, but E-selectin and ICAM-1 expression of 30 h of the Sepsis + Vehicle group (hypoinflammatory phase) was reduced markedly compared with that of the 6-h sepsis group. Moreover, there was a marked increase in E-selectin and ICAM-1 expression in small intestinal tissue of 30-h Sepsis + EX-527 versus Sepsis + Vehicle, although the expression of both of these adhesion molecules in 30-h Sepsis + EX-527 remained lower than that of the 6-h Sepsis group. These data suggest that the increased LA in EX-527 treatment is, at least partly, via endothelial cell activation in mice with sepsis. Furthermore, these data also support that one mechanism behind the beneficial effect of blocking SIRT1 is by relieving the block in expression of acute proinflammatory genes, as reported in our epigenetic analysis of the THP-1 cell model of sepsis [18].

EX-527 treatment increases PSGL-1 expression in circulating leukocytes during the hypoinflammatory phase

PSGL-1 is a ligand to E-selectin, P-selectin, and L-selectin [28, 29]. To study the effect of EX-527 on activation of circulating cells, we used whole blood flow cytometry to examine PSGL-1 expression in circulating cells in EX-527 versus Vehicle-treated mice with sepsis. The expression of PSGL-1 is expressed as a fold of control. As shown in **Fig. 7**, whereas there was no significant effect of sepsis on PSGL-1 expression on leukocytes/PMN neutrophils in early sepsis versus control, there was significantly increased expression of PSGL-1 in the leukocytes as well as PMNs in the Sepsis + EX-527 versus the Sepsis + Vehicle group. These data suggest that the increased LA in EX-527 treatment may be partly a result of an increase in PSGL-1 expression in circulating cells as well.

EX-527 enhances local innate immune responses

As SIRT1 inhibition increased LA in the microvasculature, we reasoned that EX-527 treatment (administered 24-h sepsis) in septic mice might improve the immune response by affecting the quality and number of leukocytes transgressing the mi-

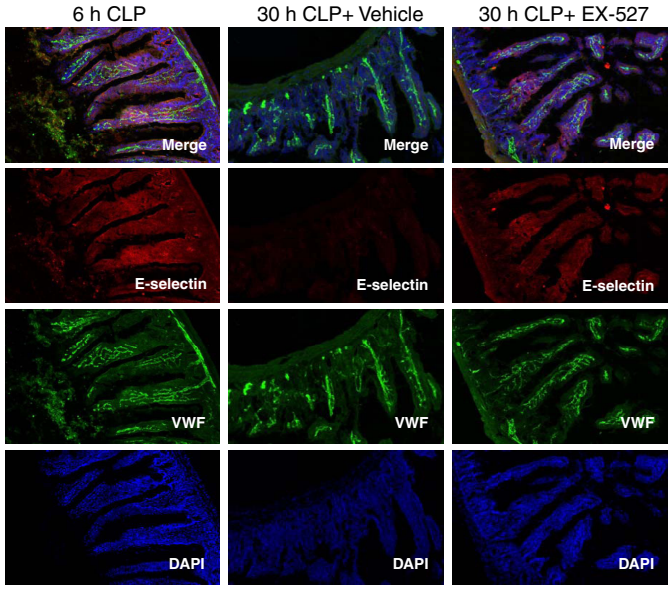

Figure 5. E-Selectin expression increased after EX-527 treatment in intestinal tissue during the hypoinflammatory phase of sepsis. Immunohistochemistry of small intestinal tissue for nuclear stain (DAPI: blue), VWF (FITC: green), E-selectin (Cy3: red), and merged color image shows that E-selectin expression increased 6-h sepsis (hyperinflammatory phase), whereas it decreased in the 30-h Sepsis + Vehicle group (hypoinflammatory phase). EX-527 treatment showed increased E-selectin expression in 30-h Sepsis + EX-527 compared with Sepsis + Vehicle, although remained lower than the 6-h sepsis group.

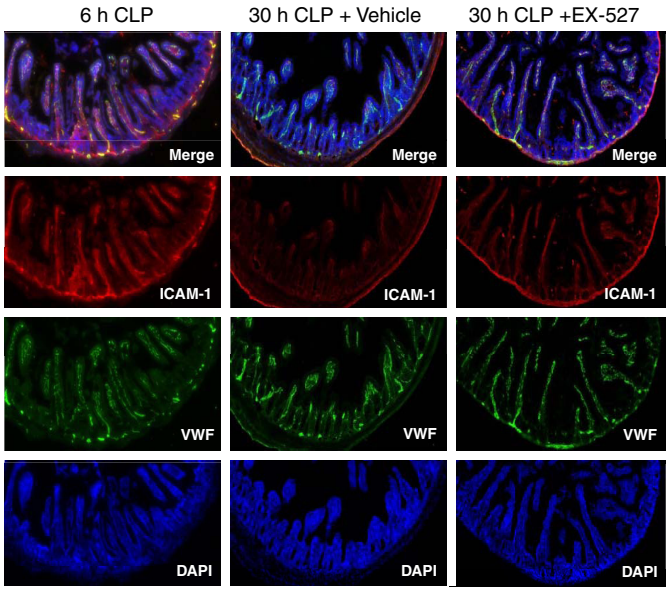

Figure 6. ICAM-1 expression increased after EX-527 treatment in intestinal tissue during the hypoinflammatory phase of sepsis. Immunohistochemistry of small intestinal tissue for nuclear stain (DAPI: blue), VWF (FITC: green), ICAM-1 (Cy3: red), and merged color image shows that ICAM-1 expression increased 6-h sepsis (hyperinflammatory phase), whereas it decreased in the 30-h Sepsis + Vehicle group (hypoinflammatory phase). EX-527 treatment showed increased ICAM-1 expression in 30-h Sepsis + EX-527 compared with Sepsis + Vehicle, although remained lower than the 6-h sepsis group.

crovessels and affecting bacterial clearance. We quantified cell populations in the peritoneum by FACS analysis (**Fig. 8A**) and found that EX-527 treatment increased F4/80+ cells (mature monocytes/macrophages) and Ly6G+/GR1+ (neutrophils; Fig. 8B and C, respectively). Importantly, EX-527 treatment (compared with vehicle) also increased Ly6C^{hi}/GR1+ cells (M1-like monocytes), which are innate immune effector cells [30], and decreased Ly6C^{lo}/GR1+ (M2-like monocytes), which are anti-inflammatory cells (Fig. 8D). This increase in the ratio of Ly6C^{hi}:Ly6C^{lo} cells in the peritoneal lavage suggests that the phenotypic change, as well as the number of leukocytes, supports the EX-527-dependent immune response recovery in septic mice.

As MVI responses and local innate immunity improved after EX-527 treatment, we reasoned that delivery of competent immune cells from microvasculature during SIRT1 inhibition might enhance bacterial clearance in the peritoneal cavity with the inciting infection. To test this, we assessed peritoneal lavage fluid for microbial growth from septic mice, with or without EX-527 treatment for 6 h or 48 h (30-h and 72-h sepsis, respectively). Peritoneal lavage fluid bacterial growth was measured after ex vivo incubation. Bacterial growth from peritoneal lavage fluid was similar in septic mice with EX-527 versus vehicle treatment for 6 h (Fig. 8E); however, bacterial growth after 48-h treatment with EX-527 was decreased markedly compared with vehicle-treated septic mice (Fig. 8F). Thus, EX-527 treatment decreases bacterial growth in the peritoneal cavity concomitant with increased delivery of effector innate immune cells, consistent with improved delivery of innate immune cells at the site of infection.

EX-527 enhances a systemic innate immune response

To investigate the systemic effect of SIRT1 inhibition in sepsis, we studied the effect of EX-527 (administered 24-h sepsis) on LPS tolerance/hypoinflammatory response in two different compartments, namely spleen and bone marrow.

EX-527 enhances the immune response in splenocytes

To study the effect of EX-527 treatment on spleen, we then examined the splenocytes from 30-h sepsis mice, with or without EX-527 treatment, which were analyzed by FACS and cytokine production in response to ex vivo LPS stimulation. In contrast to the peritoneal cavity cells, no significant differences between EX-527-treated and nontreated groups occurred in Ly6C+/GR1+ and Ly6G+/GR1+ immune cell subtype splenic populations, but F4/80+ mature macrophages decreased significantly after EX-527 treatment (data not shown). After LPS challenge, splenocytes from untreated septic mice were LPS-tolerant and showed repressed IL-1β and TNF-α mRNA levels (vs. respective Sham-control). EX-527-treated septic mice showed increased IL-1β and TNF-α mRNA levels in response to LPS stimulation (no significant difference from

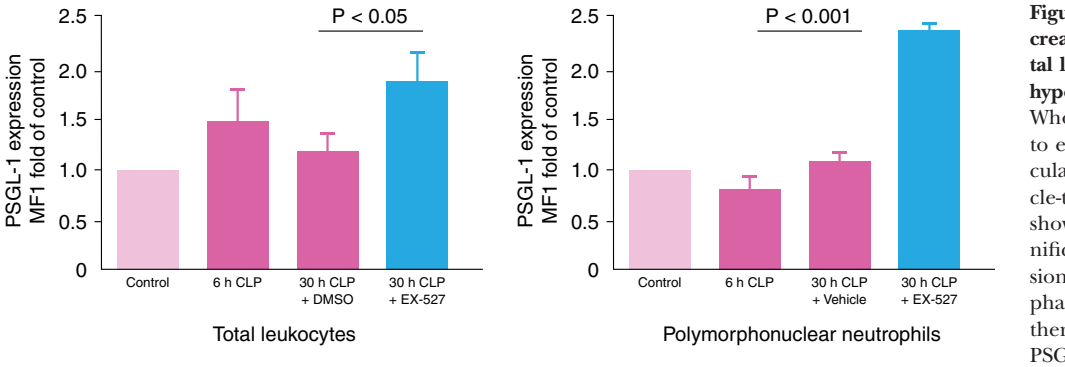

Figure 7. PSGL-1 expression increased after EX-527 treatment in total leukocytes and neutrophils in the hypoinflammatory phase of sepsis. Whole leukocyte blood flow cytometry to examine PSGL-1 expression in circulating cells in EX-527 versus Vehicle-treated mice (n=3–4/group) shows that whereas there was no significant difference in PSGL-1 expression in 6-h Sepsis (hyperinflammatory phase) compared with Sham control, there was a significant increase in PSGL-1 in the total leukocytes (all CD45-positive cells) as well as the PMN subset in the Sepsis + EX-527 group compared with the Sepsis + Vehicle group. P values are indicated in the figure.

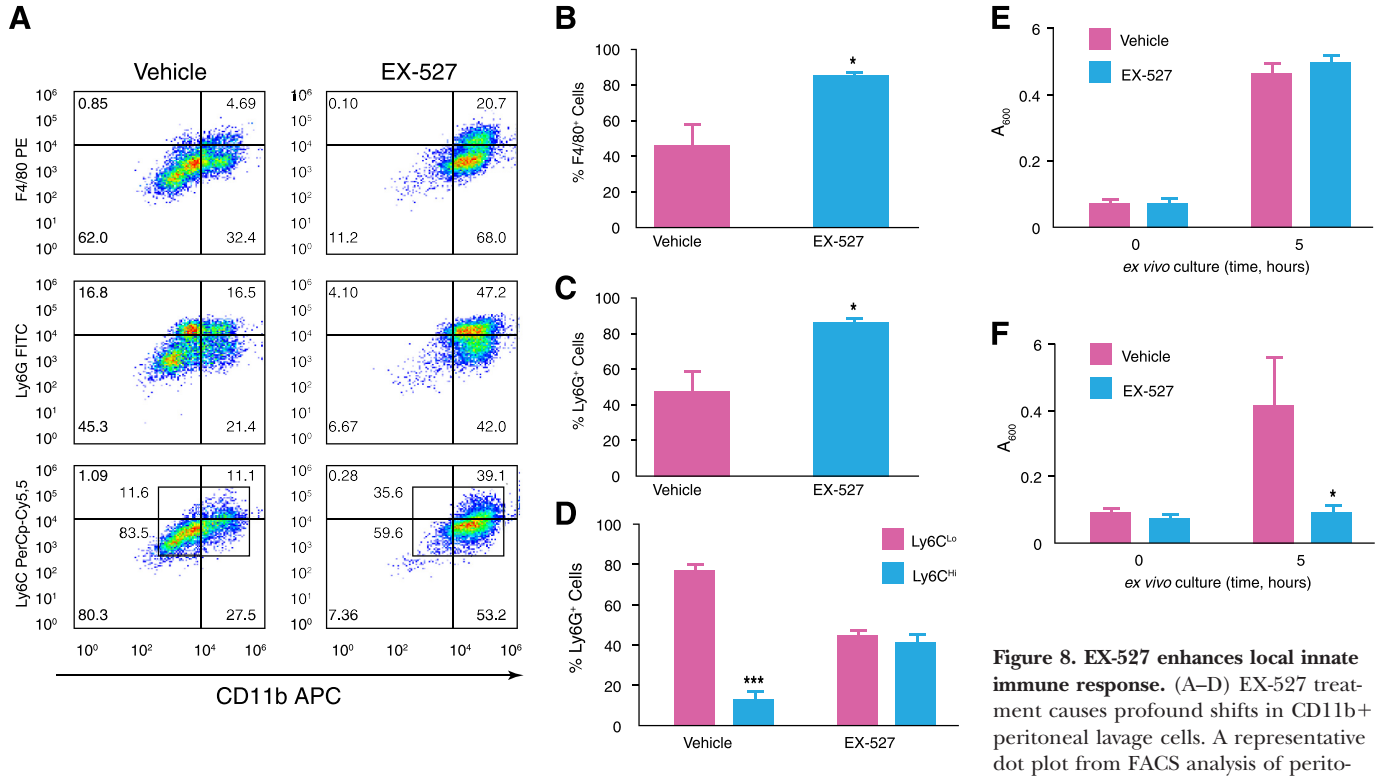

Figure 8. EX-527 enhances local innate immune response. (A–D) EX-527 treatment causes profound shifts in CD11b+ peritoneal lavage cells. A representative dot plot from FACS analysis of peritoneal lavage cells from EX-527 versus Vehicle-treated mice (n=3–4/group; A) shows that the Sepsis + EX-527 group had an increased percentage of F4/80+ (top and B; *P<0.05 vs. Sepsis+Vehicle) and Ly6G+/Gr1+ cells compared with Vehicle control (middle and C; *P<0.05 vs. Sepsis+Vehicle). There were also shifts between in Ly6C^{hi}/Gr1+ (top rectangle) and Ly6C^{lo}/Gr1+ (bottom rectangle) populations, with a shift toward increased Ly6C^{lo}/Gr1+ cells in the Sepsis + Vehicle group compared with the Sepsis + EX-527 group (bottom and D; ***P<0.0001 Ly6C^{hi}/Gr1+ vs. Ly6C^{lo}/Gr1+ in Sepsis+Vehicle mice, Tukey's post hoc analysis; error bars: SEM). (E and F) EX-527 improves bacterial clearance in the peritoneal cavity. Bacterial growth from peritoneal lavage in mice (n=4–6/group) with the Sepsis + EX-527 group was not significantly different from the Sepsis + Vehicle group in 30-h Sepsis (6-h post-treatment; E); however, there was significant reduction in bacterial growth in the Sepsis + EX-527 group compared with the Sepsis + Vehicle group in the 72-h Sepsis (48-h post-treatment) group (F). *P < 0.05 versus Sepsis + Vehicle (Student's t-test; error bars: SEM). A_{600}, Absorbance at 600 nm.

respective Sham-control; **Fig. 9A** and **B**, respectively). Thus, spleen cells from EX-527-treated septic mice restored the ability to express proinflammatory cytokines in response to LPS and reversed LPS tolerance in this important immune compartment.

EX-527 enhances immune responses in bone marrow cells

The bone marrow plays a critical role in sepsis through support of emergency production and delivery of immune cells [31]. We reasoned that EX-527 treatment might alter bone marrow-derived cells. Compared with untreated mice, bone marrow-derived Gr1+/CD11b+ cells (so called MDSCs) increased in EX-527-treated mice with sepsis (Fig. 9C). EX-527-treated septic mice (vs. vehicle) also showed increased Ly6C^{lo}/GR1+ cells and decreased Ly6C^{hi}/GR1+ cells (Fig. 9D). This shift in ratio differs from that observed in peritoneum at the site of infection (Fig. 8D). The decreased ratio of Ly6C^{hi}:Ly6C^{lo} cells in the bone marrow of EX-527-treated septic mice suggests that splenic Ly6C^{hi}/GR1+ cells were deployed to the local tissue.

Next, we purified Ly6G+/GR1+ and Ly6G−/GR1+ myeloid cells from septic mice, with and without EX-527 treatment, and examined their response to ex vivo LPS challenge by measuring TNF-α protein production. Ly6G+/GR1+ and Ly6G−/GR1+ myeloid cells from EX-527-treated mice showed a trend toward increased TNF-α protein after LPS stimulation (P=0.08 and 0.07 in Fig. 9E and F, respectively). From these data, we concluded that EX-527 administration during the hypoinflammatory phase may improve endotoxin responsiveness (reverses hypoinflammatory) in systemic innate immune cells.

SIRT1 inhibition during the immunosuppressive phase rescues mice from septic death

We tested the effect of EX-527 treatment during different phases of sepsis on mortality, predicting that early reductions in the SIRT1 counter-regulatory property would worsen outcome and that decreasing SIRT1 after it increased to drive hypoinflammation might improve mortality. We treated mice with a single i.p. dose of EX-527 (10 mg/kg i.p.) at 0 h, 12 h (hyperinflammatory phase), or 24 h (hypoinflammatory phase) after sepsis onset and followed survival. As shown in **Fig. 10**, septic mice treated with EX-527 at 0 h or 12 h had significantly decreased survival compared with sepsis alone, consistent with our earlier observations at the MVI, and in human monocytes [18], that low SIRT1 levels increase inflamma-

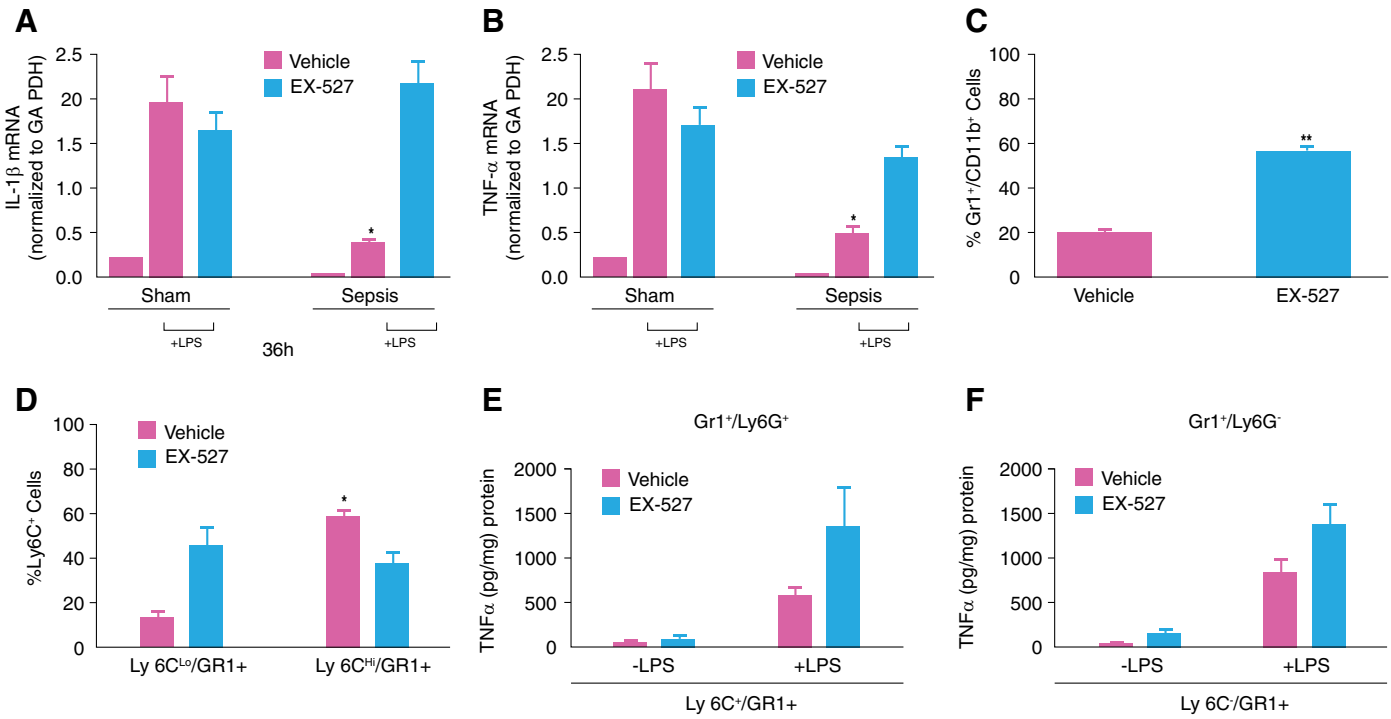

Figure 9. EX-527 treatment enhances the systemic immune response. (A–D) EX-527 enhances immune response in splenocytes. (A) LPS stimulation of splenocytes (n=3 mice/group) shows a significant increase in IL-1β mRNA expression in the Sepsis + EX-527 group, and the Sepsis + Vehicle group remained LPS-tolerant. *$P < 0.05$ versus Sham + LPS + respective treatment. (B) TNF-α mRNA expression with LPS stimulation (n=3mice/group) in Sepsis + EX-527 showed increased TNF-α mRNA expression, whereas the Sepsis + Vehicle group remained LPS-tolerant. *$P < 0.05$ versus Sham + LPS + respective treatment. (C–F) EX-527 enhances immune response in bone marrow-derived cells. (C) FACS analysis of bone marrow-derived cells (n=3 mice/group) shows a significantly increased percentage of CD11b+/Gr1+ cells in the Sepsis + EX-527 versus the Sepsis + Vehicle group. **$P < 0.01$ versus Sepsis + Vehicle. (D) Whereas there was increased percentage of Ly6C^{hi}/GR1+ cells (*P<0.05 vs. Ly6C^{lo}/GR1+) in the Sepsis + Vehicle group, there was a similar percentage of Ly6C^{hi}/GR1+ and Ly6C^{lo}/GR1+ cells in the EX-527-treated group (n=3 mice/group). (E and F) LPS stimulation of Ly6G+/GR1+ and Ly6G−/GR1+ cells from sepsis mice shows a trend toward an increase in TNF-α protein expression in Ly6G+/GR1+ and Ly6G−/GR1+ cells in the EX-527 group versus Vehicle (P=0.08 and 0.07, respectively; n=3 mice/group; Tukey's post hoc analysis; error bars: SEM).

tory response during the hyperinflammatory phase of sepsis. In marked contrast, mice treated with EX-527 during the hypoinflammatory phase (24 h), after sepsis onset, showed significant increase in survival. In the current project, we focused on the effect of EX-527 on the hypoinflammatory phase of sepsis, whereas its effect on the hyperinflammatory phase of sepsis as well as the effect of sepsis-induced mortality on MSKO mice need to be studied further. This will address an important, unanswered question of whether the decreased survival in septic mice treated with EX-527 during the hyperinflammatory phase of sepsis is a result of the effect of SIRT1 inhibition on viability of myeloid-derived cells.

DISCUSSION

This study shows that the NAD+ sensor SIRT1 broadly contributes to acute inflammation of sepsis and survival in mice. A major discovery is that SIRT1 activity regulates leukocyte-endothelial interactions in small intestinal MVI. We further demonstrate that MVI sepsis responses occur in three phases, namely hyperinflammation, hypoinflammation, and resolution of sepsis. Pharmacological inhibition of SIRT1 during the hyperinflammation phase increases LA further and decreases survival in sepsis. In striking contrast, SIRT1 inhibition after hypoinflammation sets in reverse-repressed LA (increased LA) at the MVI, increases leukocyte entry into the local infection site, improves microbial clearance, and markedly decreases mortality. Systemic improvements following SIRT1 inhibition during the hypoinflammatory phase include increased blood MAP, increased microvascular blood flow, and a shift from M2 hypoinflammatory macrophages toward M1 proinflammatory effector cells in the peritoneum, spleen, and bone marrow. Remarkably, the beneficial effect of SIRT1 on innate immune restoration during the sepsis hypoinflammatory phenotype was detected within 6 h after a single dose of EX-527. Our results are summarized in **Fig. 11**.

Our [32] and other [33] studies support that nuclear SIRT1 deacetylase activity is a critical regulator of immune and metabolic homeostasis. This study and our previous report [18] in a human promonocyte sepsis cell model show that SIRT1 levels increase during the hypoinflammatory (endotoxin tolerant) phenotype, which at the nuclear level, is determined by gener-

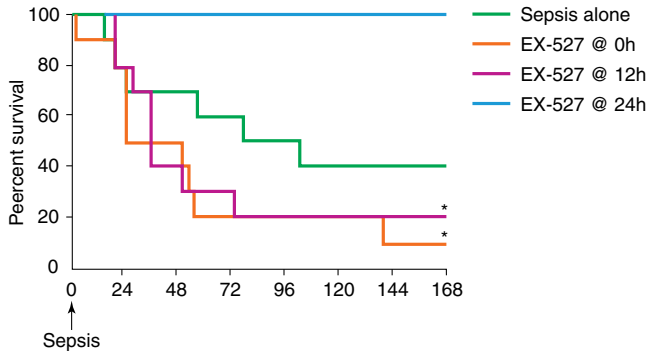

Figure 10. Kaplan-Meier survival curve with EX-527 treatment at different time-points after sepsis induction in mice. Mice received EX-527 at 0 h, 12 h, or 24 h after CLP (Sepsis), and we compared their 7-day survival. Mice without treatment had 40% survival, whereas those receiving EX-527 at 0 h and 12 h after sepsis had 10% and 20% survival, respectively. Mice receiving EX-527, 24 h after sepsis, showed 100% 7-day survival; $n = 10$ mice/group. $^*P < 0.05$ versus Sepsis alone using Log rank analysis.

ation of silent heterochromatin at the promoters of proinflammatory genes, such as TNF-α and IL-1β, whereas the euchromatin of other genes remains responsive [19]. It is known that nuclear SIRT1 counter-regulates the acute inflammatory reaction by physically interacting with NF-κB p65 to inactivate it by deacetylation, which counter-regulates specific sets of proinflammatory genes [18, 34]. Low SIRT1 levels lead to decreased inactivation of NF-κB p65 and hypersensitize many proinflammatory genes to TLR4 stimulation. In contrast, high SIRT1 levels generate repressed heterochromatin to silence proinflammatory genes, a phenotype that may persist for days [18].

If SIRT1 activity is induced before acute inflammation begins, the early hyperinflammatory phase is muted [35]. SIRT1 also balances mitochondrial glucose and fatty acid oxidation in human and murine phagocytes [17, 36]. Thus, SIRT1 acts as a checkpoint of immune and metabolic homeostasis [37].

The SIRT1 inhibitor used in this study, a small molecule EX-527, is a noncompetitive SIRT1 inhibitor with high specificity for the NAD+-binding pocket, thereby limiting deacetylation of target proteins and histones [38]. The effects of this agent were remarkably quick and appeared to extend for up to 48 h after a single dose. In this study, our immunohistochemistry results suggested that EX-527 might result in decreased levels of SIRT1, which is not expected from its properties [35, 38]. To examine further whether EX-527 lowers the SIRT1 levels, as well as blocking its deacetylation effect, we performed immunoblots (Fig. 2B). SIRT1 levels using immunoblots were not decreased by EX-527, a finding similar to our studies in human THP-1 cells [18].

Mechanistically, this study supports that SIRT1 inhibition during the hypoinflammatory phase may reverse the repressed LA by restoring activation of E-selectin and ICAM-1 expression at the MVI. Moreover, SIRT1 inhibition shifts in the M2 repressor toward the M1 effector monocyte/macrophage phenotypes in the spleen and peritoneal cavity and increases accumulation of neutrophils. As all of these processes are regulated, at least in part by NF-κB, one biochemical mechanism responsible for SIRT1 inhibition might be to reverse deacetylation of NF-κB p65 transactivator; however, we have been unable to measure acetylation of p65 S310 in the tissue. As a broad guardian of homeostasis and regulator of multiple proteins, histones, and genes, inhibition of sustained increases in SIRT1 expression could improve sepsis resolution by several

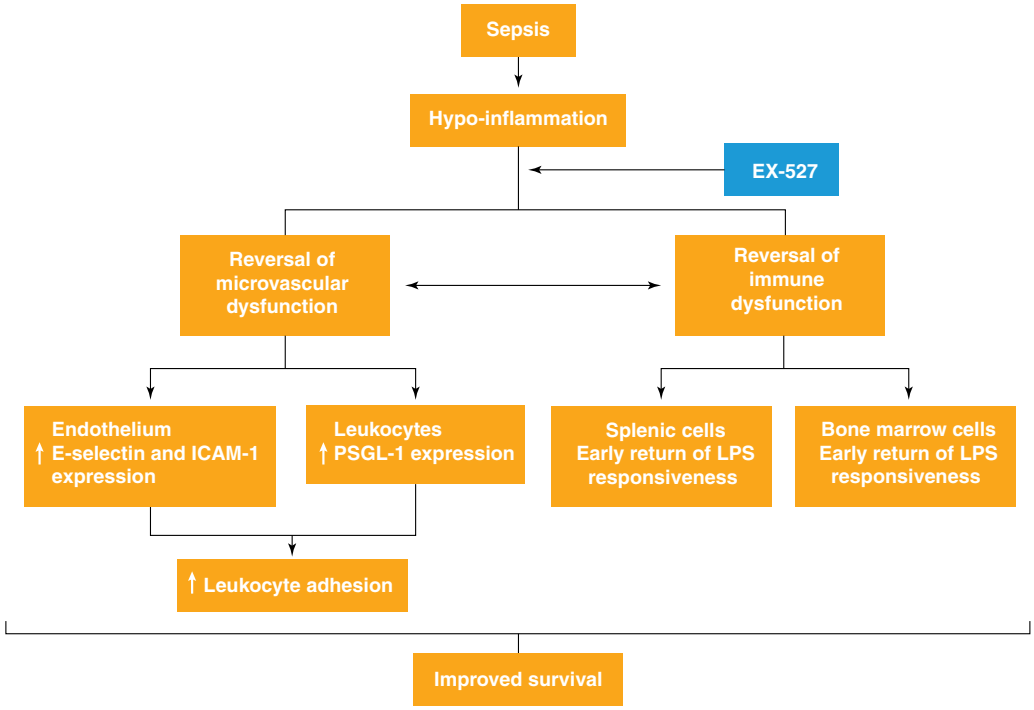

Figure 11. EX-527 treatment during the hypoinflammatory phase of sepsis. In this project, we show that EX-527 treatment during the hypoinflammatory phase of sepsis reverses microvascular dysfunction via activation of endothelial and circulating cells. EX-527 treatment during the hypoinflammatory phase also reverses immune dysfunction. Reversal of microvascular and immune dysfunction improves survival in rodent sepsis.

concomitant cellular processes that collectively rebalance immunity, metabolism, and mitochondrial bioenergetics. We are exploring such possibilities.

Our results also emphasize the need to understand better the MVI during all phases of sepsis. For example, barrier dysfunction of MVI impacts multiple organs [26, 39, 40]. The SIRT1 activator resveratrol decreases blood brain barrier dysfunction in chronic neurodegenerative disorders [41, 42], but there are no studies, to our knowledge, that focus on the role of SIRT1 on the barrier dysfunction in sepsis.

Whereas results of this study support the accumulating importance of SIRT1, a fundamentally important contributor to balancing the inflammatory and innate immune responses and their connection with metabolism and bioenergetics [17, 36], further study is needed to clarify molecular and physiologic mechanisms. Important, unanswered questions in need of further study include: (1) whether general or MSKO mice are at higher risk for early sepsis death; (2) whether conditional and cell-specific knockout constructs will genetically support sepsis rescue during the adaptive or endotoxin-tolerant sepsis phase; (3) whether physiologic changes in the MVI primarily involve neutrophils and/or monocytes/macrophages; and (4) whether augmented immune balance to improve late sepsis outcome also involves and/or depends on changes in metabolism and bioenergetics.

In conclusion, we introduce a new way to reduce mortality during sepsis hypoinflammation and immunosuppression, a concept of emerging significance [3, 7]. New approaches are timely, as the incidence of sepsis is rising worldwide, and death occurs in approximately one in four of the more than 1 million sepsis hospitalizations in the United States each year [3, 43]. We also show the importance of MVI in sequentially directing the course of sepsis. Taken together, our results support the significance of the SIRT1 NAD+ axis and checkpoint for maintaining whole-body homeostasis and introduce a new way to treat sepsis.

AUTHORSHIP

V.T.V. and C.E.M. provided the concept and design. N.L.B. and J.D.W. generated the data. T.F.L., C.M.B., X.W., N.L.B., J.D.W., B.K.Y., V.T.V., and C.E.M. gave the analysis and interpretation. V.T.V., C.E.M., and B.K.Y. generated the manuscript.

ACKNOWLEDGMENTS

This work was supported by the following U.S. National Institutes of Health grants: K08GM086470 and R01GM099807 (to V.T.V.), R01AI065791 and R01AI079144 (to C.E.M.), and NS081014 and R01AI079144-S1 (principal investigator: C.E.M.; to C.M.B.). We thank Dr. Hang Shi (Georgia State University, Atlanta, GA, USA) for MSKO, Dr. Werner Bischoff (Wake Forest School of Medicine, Winston-Salem, NC, USA) for microbiological support, Dr. Christopher Peters (Wake Forest School of Medicine) for support for immunohistochemistry, and Sue Cousart and Catherine Brewer for technical support.

DISCLOSURES

The authors declare no conflicts of interest.

REFERENCES

1. Gaieski, D. F., Edwards, J. M., Kallan, M. J., Carr, B. G. (2013) Benchmarking the incidence and mortality of severe sepsis in the United States. *Crit. Care Med.* **41,** 1167–1174.
2. Hotchkiss, R. S., Karl, I. E. (2003) The pathophysiology and treatment of sepsis. *N. Engl. J. Med.* **348,** 138–150.
3. Hotchkiss, R. S., Opal, S. (2010) Immunotherapy for sepsis—a new approach against an ancient foe. *N. Engl. J. Med.* **363,** 87–89.
4. Williams, S. C. (2012) After Xigris, researchers look to new targets to combat sepsis. *Nat. Med.* **18,** 1001.
5. Boomer, J. S., To, K., Chang, K. C., Takasu, O., Osborne, D. F., Walton, A. H., Bricker, T. L., Jarman, S. D., 2nd, Kreisel, D., Krupnick, A. S., et al. (2011) Immunosuppression in patients who die of sepsis and multiple organ failure. *JAMA* **306,** 2594–2605.
6. Brahmamdam, P., Inoue, S., Unsinger, J., Chang, K. C., McDunn, J. E., Hotchkiss, R. S. (2010) Delayed administration of anti-PD-1 antibody reverses immune dysfunction and improves survival during sepsis. *J. Leukoc. Biol.* **88,** 233–240.
7. Chang, K., Svabek, C., Vazquez-Guillamet, C., Sato, B., Rasche, D., Wilson, S., Robbins, P., Ulbrandt, N., Suzich, J., Green, J., et al. (2014) Targeting the programmed cell death 1: programmed cell death ligand 1 pathway reverses T cell exhaustion in patients with sepsis. *Crit. Care.* **18,** R3.
8. Hotchkiss, R. S., Tinsley, K. W., Swanson, P. E., Grayson, M. H., Osborne, D. F., Wagner, T. H., Cobb, J. P., Coopersmith, C., and Karl, I. E. (2002) Depletion of dendritic cells, but not macrophages, in patients with sepsis. *J. Immunol.* **168,** 2493–2500.
9. Aird, W. C. (2003) The role of the endothelium in severe sepsis and multiple organ dysfunction syndrome. *Blood* **101,** 3765–3777.
10. Granger, D. N., Kubes, P. (1994) The microcirculation and inflammation: modulation of leukocyte-endothelial cell adhesion. *J. Leukoc. Biol.* **55,** 662–675.
11. Vachharajani, V., Russell, J. M., Scott, K. L., Conrad, S., Stokes, K. Y., Tallam, L., Hall, J., Granger, D. N. (2005) Obesity exacerbates sepsis-induced inflammation and microvascular dysfunction in mouse brain. *Microcirculation* **12,** 183–194.
12. Skibsted, S., Jones, A. E., Puskarich, M. A., Arnold, R., Sherwin, R., Trzeciak, S., Schuetz, P., Aird, W. C., Shapiro, N. I. (2013) Biomarkers of endothelial cell activation in early sepsis. *Shock* **39,** 427–432.
13. Beeson, P. B. (1947) Tolerance to bacterial pyrogens: I. factors influencing its development. *J. Exp. Med.* **86,** 29–38.
14. Chen, X., El Gazzar, M., Yoza, B. K., McCall, C. E. (2009) The NF-κB factor RelB and histone H3 lysine methyltransferase G9a directly interact to generate epigenetic silencing in endotoxin tolerance. *J. Biol. Chem.* **284,** 27857–27865.
15. Cavaillon, J. M., Adrie, C., Fitting, C., Adib-Conquy, M. (2003) Endotoxin tolerance: is there a clinical relevance? *J. Endotoxin Res.* **9,** 101–107.
16. Cross, A. S. (2002) Endotoxin tolerance-current concepts in historical perspective. *J. Endotoxin Res.* **8,** 83–98.
17. Liu, T. F., Vachharajani, V. T., Yoza, B. K., McCall, C. E. (2012) NAD+-dependent sirtuin 1 and 6 proteins coordinate a switch from glucose to fatty acid oxidation during the acute inflammatory response. *J. Biol. Chem.* **287,** 25758–25769.
18. Liu, T. F., Yoza, B. K., El Gazzar, M., Vachharajani, V. T., McCall, C. E. (2011) NAD+-dependent SIRT1 deacetylase participates in epigenetic reprogramming during endotoxin tolerance. *J. Biol. Chem.* **286,** 9856–9864.
19. McCall, C. E., Yoza, B., Liu, T., El Gazzar, M. (2010) Gene-specific epigenetic regulation in serious infections with systemic inflammation. *J. Innate Immun.* **2,** 395–405.
20. Dietrich, M. O., Antunes, C., Geliang, G., Liu, Z. W., Borok, E., Nie, Y., Xu, A. W., Souza, D. O., Gao, Q., Diano, S., et al. (2010) Agrp neurons mediate Sirt1's action on the melanocortin system and energy balance: roles for Sirt1 in neuronal firing and synaptic plasticity. *J. Neurosci.* **30,** 11815–11825.
21. Ayala, A., Kisala, J. M., Felt, J. A., Perrin, M. M., Chaudry, I. H. (1992) Does endotoxin tolerance prevent the release of inflammatory monokines (interleukin 1, interleukin 6, or tumor necrosis factor) during sepsis? *Arch. Surg.* **127,** 191–196, discussion 196–197.
22. Singer, G., Stokes, K. Y., Terao, S., Granger, D. N. (2009) Sepsis-induced intestinal microvascular and inflammatory responses in obese mice. *Shock* **31,** 275–279.
23. Tailor, A., Granger, D. N. (2003) Hypercholesterolemia promotes P-selectin-dependent platelet-endothelial cell adhesion in postcapillary venules. *Arterioscler. Thromb. Vasc. Biol.* **23,** 675–680.
24. Tsujikawa, A., Kiryu, J., Nonaka, A., Yamashiro, K., Nishiwaki, H., Honda, Y., Ogura, Y. (2000) Leukocyte-endothelial cell interactions in diabetic retina after transient retinal ischemia. *Am. J. Physiol. Regul. Integr. Comp. Physiol.* **279,** R980–R989.

25. Wang, X., Yang, Z., Xue, B., Shi, H. (2011) Activation of the cholinergic antiinflammatory pathway ameliorates obesity-induced inflammation and insulin resistance. *Endocrinology* **152,** 836–846.
26. Vachharajani, V., Cunningham, C., Yoza, B., Carson, J. Jr., Vachharajani, T. J., McCall, C. (2012) Adiponectin-deficiency exaggerates sepsis-induced microvascular dysfunction in the mouse brain. *Obesity* **20,** 498–504.
27. Gillum, M. P., Kotas, M. E., Erion, D. M., Kursawe, R., Chatterjee, P., Nead, K. T., Muise, E. S., Hsiao, J. J., Frederick, D. W., Yonemitsu, S., et al. (2011) SirT1 regulates adipose tissue inflammation. *Diabetes* **60,** 3235–3245.
28. Patel, K. D., Moore, K. L., Nollert, M. U., McEver, R. P. (1995) Neutrophils use both shared and distinct mechanisms to adhere to selectins under static and flow conditions. *J. Clin. Invest.* **96,** 1887–1896.
29. Asa, D., Raycroft, L., Ma, L., Aeed, P. A., Kaytes, P. S., Elhammer, A. P., Geng, J. G. (1995) The P-selectin glycoprotein ligand functions as a common human leukocyte ligand for P- and E-selectins. *J. Biol. Chem.* **270,** 11662–11670.
30. Olefsky, J. M., Glass, C. K. (2010) Macrophages, inflammation, and insulin resistance. *Ann. Rev. Physiol.* **72,** 219–246.
31. Nagai, Y., Garrett, K. P., Ohta, S., Bahrun, U., Kouro, T., Akira, S., Takatsu, K., Kincade, P. W. (2006) Toll-like receptors on hematopoietic progenitor cells stimulate innate immune system replenishment. *Immunity* **24,** 801–812.
32. Liu, T. F., Brown, C. M., El Gazzar, M., McPhail, L., Millet, P., Rao, A., Vachharajani, V. T., Yoza, B. K., McCall, C. E. (2012) Fueling the flame: bioenergy couples metabolism and inflammation. *J. Leukoc. Biol.* **92,** 499–507.
33. Kauppinen, A., Suuronen, T., Ojala, J., Kaarniranta, K., Salminen, A. (2013) Antagonistic crosstalk between NF-κB and SIRT1 in the regulation of inflammation and metabolic disorders. *Cell. Signal.* **25,** 1939–1948.
34. Yeung, F., Hoberg, J. E., Ramsey, C. S., Keller, M. D., Jones, D. R., Frye, R. A., Mayo, M. W. (2004) Modulation of NF-κB-dependent transcription and cell survival by the SIRT1 deacetylase. *EMBO J.* **23,** 2369–2380.
35. Yang, H., Zhang, W., Pan, H., Feldser, H. G., Lainez, E., Miller, C., Leung, S., Zhong, Z., Zhao, H., Sweitzer, S., et al. (2012) SIRT1 activators suppress inflammatory responses through promotion of p65 deacetylation and inhibition of NF-κB activity. *PLoS One* **7,** e46364.
36. Vats, D., Mukundan, L., Odegaard, J. I., Zhang, L., Smith, K. L., Morel, C. R., Wagner, R. A., Greaves, D. R., Murray, P. J., Chawla, A. (2006) Oxidative metabolism and PGC-1β attenuate macrophage-mediated inflammation. *Cell. Metab.* **4,** 13–24.
37. Canto, C., Jiang, L. Q., Deshmukh, A. S., Mataki, C., Coste, A., Lagouge, M., Zierath, J. R., Auwerx, J. (2010) Interdependence of AMPK and SIRT1 for metabolic adaptation to fasting and exercise in skeletal muscle. *Cell. Metab.* **11,** 213–219.
38. Gertz, M., Fischer, F., Nguyen, G. T., Lakshminarasimhan, M., Schutkowski, M., Weyand, M., Steegborn, C. (2013) Ex-527 inhibits sirtuins by exploiting their unique NAD+-dependent deacetylation mechanism. *Proc. Natl. Acad. Sci. USA* **110,** E2772–E2781.
39. Hofer, S., Bopp, C., Hoerner, C., Plaschke, K., Faden, R. M., Martin, E., Bardenheuer, H. J., Weigand, M. A. (2008) Injury of the blood brain barrier and up-regulation of ICAM-1 in polymicrobial sepsis. *J. Surg. Res.* **146,** 276–281.
40. Jeppsson, B., Freund, H. R., Gimmon, Z., James, J. H., von Meyenfeldt, M. F., Fischer, J. E. (1981) Blood-brain barrier derangement in sepsis: cause of septic encephalopathy? *Am. J. Surg.* **141,** 136–142.
41. Chang, H. C., Tai, Y. T., Cherng, Y. G., Lin, J. W., Liu, S. H., Chen, T. L., Chen, R. M. (2014) Resveratrol attenuates high-fat diet-induced disruption of the blood-brain barrier and protects brain neurons from apoptotic insults. *J. Agric. Food Chem.* **62,** 3466–3475.
42. Potter, K. A., Buck, A. C., Self, W. K., Callanan, M. E., Sunil, S., Capadona, J. R. (2013) The effect of resveratrol on neurodegeneration and blood brain barrier stability surrounding intracortical microelectrodes. *Biomaterials* **34,** 7001–7015.
43. Angus, D. C. (2011) The search for effective therapy for sepsis: back to the drawing board? *JAMA* **306,** 2614–2615.

KEY WORDS:
immunosuppression · chromatin remodeling · endotoxin tolerance